

Experimental and Analytical Study of Jet Noise Modeling

L. F. MOON* AND S. W. ZELAZNY†
Bell Aerospace Division of Textron, Buffalo, N.Y.

Detailed turbulence profiles were measured at 28 axial locations extending from the nozzle exit to 12 nozzle diameters downstream for a circular jet exhausting into an ambient environment. Measurements include mean velocity, turbulence intensity, shear stress, as well as sound intensity, spectral distribution, and directivity. A noise model was developed which accurately predicted sound amplitude, spectral distribution, and directivity pattern in terms of self and shear noise components. A turbulence model was also developed which accurately predicted mean velocity, turbulence intensity, and shear stress in axisymmetric jets with predictions starting in the potential core. Turbulence and noise models were computationally coupled and the sensitivity of noise predictions to inaccuracies in the predicted turbulence field studied. It is shown that errors of only 20% in predicted peak turbulence intensity level in the core region results in up to a 5-db difference in the predicted over-all sound pressure level.

Nomenclature

a	= jet radius
a_o	= speed of sound
f	= ratio of v^2/u^2 , specified empirically
i	= sound intensity
l_i	= fourth-order length scale, $\int_0^r R_{ijij}(\eta, \xi, o) d\xi_i$
l_s	= shear layer half width
M	= Mach number
M_c	= convection Mach number
R	= distance from nozzle exit to observer
R_{ijkl}	= fourth-order correlation coefficient, $\langle u_i u_j(\eta, o) u_k u_l(\xi, o) \rangle / \langle u_i u_j(\eta, o) u_k u_l(\eta, o) \rangle$
r	= radial coordinate
r_1, r_2	= inner and outer edges of the mixing region, Fig. 1
r_{1u}	= half width of the shear layer in the core region
t	= time, moving frame of reference
U	= instantaneous or mean axial velocity
U_i	= instantaneous velocity
U_j	= jet velocity at exit
u_i	= turbulent velocity
u'	= rms value of longitudinal fluctuating component
V	= eddy volume
v'	= rms value of transverse fluctuating component
x_i	= coordinates (tensor)
$ x $	= distance from eddy to observer
α, β, γ	= constants
ε	= eddy viscosity
ζ	= defined by Eq. (10)
η, ξ	= points of evaluation in eddy
θ	= angle defined in Fig. 1
ρ	= density
T_{ij}	= $\rho U_i U_j + P_{ij} - a_o^2 \rho \delta_{ij}$
τ	= time, fixed frame of reference
ψ	= angle defined in Fig. 1
ω	= radian frequency
$\langle \rangle$	= time averaged quantity

Subscripts

1	= evaluated in axial direction
2	= evaluated in transverse direction
c	= value at centerline
e	= value at freestream
o	= evaluated at far field conditions

Presented as Paper 74-3 at the AIAA 12th Aerospace Sciences Meeting, Washington, D.C., January 30–February 1, 1974; submitted February, 7, 1974; revision received August 5, 1974. This work was supported in part by the Air Force Office of Scientific Research under Contract F44620-70-C-0116 with technical monitoring by B. T. Wolfson and under a Bell Aerospace Company IR&D program.

Index categories: Aircraft Noise, Aerodynamics (Including Sonic Boom); Jets, Wakes, and Viscid-Inviscid Flow Interactions.

* Principal Scientist, High Energy Laser Technology.

† Research Scientist, Computational Fluid and Continuum Mechanics. Member AIAA.

r = evaluated in radial direction
 se = evaluated for self noise
 sh = evaluated for shear noise
 u = value at velocity half width
 x = evaluated in direction of observation

Introduction

THE ability to theoretically predict complex turbulent jet flows and acoustic fields is important when seeking to optimize jet engine performance while minimizing noise generation. Before such predictions can be made, it is necessary to model both the turbulence and the sound. That is, it is necessary to first obtain a description of the flowfield using a turbulence model and then estimate the aerodynamic noise using the appropriate aerodynamic parameters in the sound model.

The theory of aerodynamic noise began with Lighthill's two classic papers^{1,2} on the subject. During the more than two decades since the original formulation a considerable amount of effort, both theoretical and experimental, has been expended in an attempt to more accurately estimate the sound produced from turbulent flows, in particular, from turbulent jets. However, at least two questions remain: 1) have the sound generation mechanisms been modeled in terms of the appropriate turbulence parameters (velocity and velocity gradients, turbulence intensity, length, and time scales, etc.) and 2) can these flow parameters be predicted with sufficient accuracy, i.e., a degree of accuracy which allows useful estimates to be obtained for the sound radiated from the flow given an accurate sound model?

The objective of the experimental and analytical investigation reported herein was to determine the sensitivity of noise level predictions to inaccuracies in the predicted turbulent flowfield parameters used in the sound model. Figure 1 shows a schematic

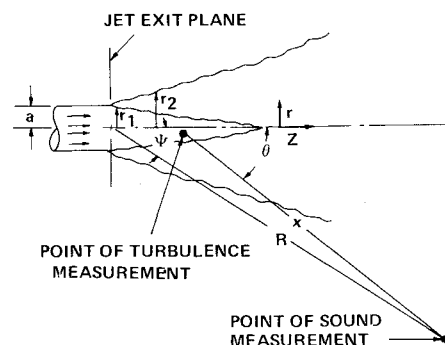


Fig. 1 Schematic of axisymmetric jet and coordinate system used to designate point of sound observation.

of the axisymmetric jet considered and the coordinate system used in designating the sound observation point in the far field. In Sec. II, a sound model is developed and a description of the detailed experimental jet data obtained in this investigation is presented. Empirical models for eddy viscosity and turbulence intensity are presented in Sec. III. and shown to give good agreement with the jet mixing data used as standard test cases at the NASA Workshop on Free Turbulent Shear Flows.³ In Sec. IV the sound and turbulence models were computationally coupled and predictions made for the velocity, turbulence intensity, and sound pressure levels. The sensitivity of sound pressure level predictions to inaccuracies in the initial turbulence intensity profiles were examined.

Sound Model

Background

Lighthill's approach to the problem of aerodynamic sound production is an "exactly valid one."^{1,2,4} It assumes that the flow in a given region changes at a rate equal to the total inward normal momentum and that the momentum changes at a rate equal to the total inward normal component of the complex stress system. It makes no simplifying assumption concerning the shear stresses and their relation to rates of strain. His formulation includes: 1) the sound generation mechanism, 2) convection of sound with the flow, and 3) sound dissipation by conduction and viscosity. Having an exact formulation of the problem, however, does not guarantee an exact solution as is evidenced by the inexactness with which aerodynamic sound can be predicted some twenty years after the formulation of the problem and after much experimental and theoretical work by many researchers. Lighthill demonstrated that for aerodynamic sound generation the equations of continuity and momentum could be cast in the form of nonhomogeneous wave equation for which a solution exists. However, the solution is in terms of covariances which are very difficult to measure or estimate. It is this point that has led to many of the discrepancies in the prediction of sound produced by jets. Realizing these difficulties, Lighthill turned to a dimensional analysis argument in a first attempt to deduce the dependence of the radiated sound on the fluctuating flowfield. His arguments led to a now famous $\langle U \rangle^8$ law, where $\langle U \rangle$ is the bulk jet exit velocity. This law, although a very useful empirical relationship, masks the dependence of the sound generation on the turbulence structure.

Derivation

We first sketch the classical derivation in order to clarify the differences which have allowed the present improvement in the acoustic modeling. The classical theory of the physical mechanism of noise generated by turbulent air flows as formulated by Lighthill¹ is:

$$(\partial^2 \rho / \partial t^2) - a_0^2 (\partial^2 \rho / \partial x_i \partial x_i) = \partial^2 T_{ij} / \partial x_i \partial x_j \quad (1)$$

The lefthand side of this equation describes the propagation of sound in a medium at rest, and the righthand side is a collection of source terms. Expressing the source term identified by Lighthill in the conventional manner of turbulence theory (i.e., dividing the velocity-field into a mean and a fluctuating part), Csanady⁵ showed the source term was composed of terms containing not only turbulence parameters, which had previously been identified, but also terms containing mean velocity gradient. A short time later Jones,⁶ working with Csanady, identified a term containing the second derivative of mean velocity. Thus, the forcing function representing the generation of aerodynamic noise was shown to be dependent upon several different mechanisms: fluctuating shear stress interactions with 1) themselves, 2) the first derivative of mean velocity, and 3) the second derivative of mean velocity. Jones concluded that at least for a round jet only the first two of these are of any practical significance, with the second one possibly dominant.

Dividing the velocity field into a mean and a fluctuating part (i.e., $U_i = \langle U_i \rangle + u_i$) and assuming an idealized mixing

layer characterized by $\langle U_1 \rangle = \langle U_1(x_2, x_3) \rangle$ and $\langle U_2 \rangle = \langle U_3 \rangle = 0$.⁷ Eq. (2) can be transformed to:

$$(\partial^2 \rho / \partial t^2) - a_0^2 (\partial^2 \rho / \partial x_i \partial x_i) = S' \quad (2)$$

where S' is given by:

$$S' = \frac{\partial^2}{\partial x_i \partial x_j} (\rho u_i u_j) + 2 \frac{\partial \langle U \rangle}{\partial x_j} \frac{\partial}{\partial x_i} (\rho u_j) \quad (3)$$

Equation (2) is the ordinary wave equation for which the solution is known. The first term on the right side of Eq. (3) is called the self noise since it involves only turbulence quantities. The second term is called shear noise since it is dependent on the gradient of the mean velocity as well as turbulence quantities.⁸

The solution of Eq. (2) for the first term in Eq. (3) yields the intensity of the self noise generated from a unit volume of turbulence,⁹⁻¹¹

$$i_{se} = \int_V \frac{\rho^2}{16\pi^2 |x|^2 \rho_0 a_0^5} \frac{\partial^4}{\partial \tau^4} \langle u_x^2(\eta, 0) u_x^2(\xi, \tau) \rangle dV \quad (4)$$

and the solution for the second term gives the intensity of the shear noise generated from the same turbulence volume.^{5,12,13}

$$i_{sh} = \int_V \frac{\rho^2 \cos^4 \theta}{4\pi^2 |x|^2 \rho_0 a_0^5} \left(\frac{\partial \langle U \rangle}{\partial r} \right)^2 \frac{\partial^2}{\partial \tau^2} \langle u_1 u_r(\eta, 0) u_1 u_r(\xi, \tau) \rangle dV + \int_V \frac{\rho^2 \sin^2 \theta \cos^2 \theta}{4\pi^2 |x|^2 \rho_0 a_0^5} \left(\frac{\partial \langle U \rangle}{\partial r} \right)^2 \frac{\partial^2}{\partial \tau^2} \langle u_r u_r(\eta, 0) u_r u_r(\xi, \tau) \rangle dV \quad (5)$$

Many assumptions and simplifications have been made in arriving at these results and these as well as the details of the solution can be found in the cited references.

The total intensity of self noise plus shear noise, before allowance is made for the effects of convection and refraction, reaching the far field due to a unit volume of turbulence is given by combining Eqs. (4) and (5). The radiation due to self noise depends on the second time derivative; whereas the shear noise radiation depends on the first time derivative; thus the self noise should radiate at a higher characteristic frequency than the shear noise. The directivity associated with the shear noise causes the high-frequency self noise to dominate toward the sides of a jet, and the lower frequency shear noise to dominate ahead and behind the jet.

Convection of eddy sound sources by the mean flow has been discussed by many authors and different convection factors have been identified for each sound generating mechanism. The convection factor for self noise as given by Lighthill¹ and modified by Ffowcs Williams⁹ and Ribner^{10,11} for a moving frame of reference is $[(1 - M_c \cos \theta)^2 + \alpha_{se}^2]^{-5/2}$. The convection factor for shear noise as given by Jones⁸ and modified to eliminate the singularity at $1 - M_c \cos \theta = 0$ following Ribner for a moving frame of reference is $[(1 - M_c \cos \theta)^2 + \alpha_{sh}^2 M_c^2]^{-3/2}$. The effect of mean flow convection is to increase the sound intensity in the downstream direction.

Refraction of eddy sound sources by the jet flow bends the sound rays away from the jet axis; thus, weakening the sound along the core and causing a so-called zone of silence along the jet axis. Effects of refraction increase with increasing frequency. Schubert¹⁴ has suggested that jet noise directivity at a particular frequency can be obtained by first computing directivity due to self noise and shear noise with convection, then multiplying by a refraction factor. The form of this factor is as yet unknown; fortunately, for observation angles greater than 20° this factor may be neglected.

Combining Eqs. (4) and (5) with the convection factors and neglecting refraction, one arrives at an expression for the sound intensity in the far field due to a unit volume of turbulence:

$$i_t = \int_V \frac{\rho^2}{16\pi^2 |x|^2 \rho_0 a_0^5} \frac{\partial^4}{\partial \tau^4} \langle (u_x^2)^2 \rangle R_{xxxx} dV \times \frac{1}{[(1 - M_c \cos \theta)^2 + \alpha_{se}^2 M_c^2]^{5/2}} + \int_V \frac{\rho^2}{4\pi^2 |x|^2 \rho_0 a_0^5} \left(\frac{\partial \langle U \rangle}{\partial r} \right)^2 \frac{\partial^2}{\partial \tau^2} \langle (u_1 u_r)^2 \rangle R_{1r1r} dV \times$$

$$\frac{\cos^4 \theta}{[(1 - M_c \cos \theta)^2 + \alpha_{sh} M_c^2]^{3/2}} + \int_V \frac{\rho^2}{4\pi^2 |x|^2 \rho_o a_o^5} \left(\frac{\partial \langle U \rangle}{\partial r} \right)^2 \frac{\partial^2}{\partial t^2} \langle (u_r^2)^2 \rangle R_{rrrr} dV \times \frac{\sin^2 \theta \cos^2 \theta}{[(1 - M_c \cos \theta)^2 + \alpha_{sh}^2 M_c^2]^{3/2}} \quad (6)$$

where the covariances have been written in terms of correlation coefficients. The sound generation mechanisms and directivity patterns described by this equation are applicable to circular, coannular, and two-dimensional jets. The derivation of Eq. (6) has followed strictly classical methods and assumptions. It represents an important result in that it includes explicitly the self (first) and shear (second and third) noise terms with their different intensities and directives, and clearly shows the relationship of these sound producing mechanisms to the mean and turbulence properties of the flow.

It appears at this point that the mechanisms for aerodynamic sound generation from a unit volume of turbulence are quite well understood; however, the solutions of the Lighthill wave equation with this complicated forcing function still contain very complicated second- and fourth-time derivatives of two-point turbulence correlations. As yet, these derivatives cannot be predicted directly and must therefore be written in terms of predictable turbulence quantities. To simplify this equation, reasonable approximations, based on turbulence measurements, must be made. Many researchers have contributed to our understanding of the correlations and how they can be modeled.¹⁴⁻²³

We will now discuss our approach to the solution of Eq. (6) which permits sound radiation to be accurately estimated from measured flow quantities without the requirement of high order differentiation of measured data. In modeling the very complicated integrals in the preceding equation, the following assumptions were made. 1) Each eddy radiates at two characteristic frequencies, one corresponding to the quadrupole radiation (self noise), and one corresponding to dipole radiation (shear noise). 2) The time dependence of the sound produced from each eddy can be written in terms of these characteristic frequencies. 3) Three orthogonal length scales, two about equal in length and a third about twice as long are associated with each sound producing eddy. 4) The characteristic frequencies can be written in terms of these length scales, the length scale in the direction of the flow being characteristic of the shear noise and transverse length scale being characteristic of the self noise. 5) The volume of each sound producing eddy can be characterized by a constant times the product of these characteristic orthogonal length scales. 6) The velocity fluctuations are normally distributed throughout each eddy. 7) Each sound producing eddy radiates independently of the surrounding eddies.

Some of the forementioned assumptions are not, at least for the present, supported by the mathematical rigor that one would like; however, they can be justified by heuristic arguments. Lighthill,¹ in analyzing his sound theory suggested that the time dependence could be expressed in terms of a characteristic frequency. Re-examination of the sound generation mechanisms indicate that, if Lighthill's suggestion is appropriate, the time dependence must be expressed in terms of at least two characteristic frequencies or times: one frequency corresponding to the self noise and a second corresponding to the shear noise. This assumption does not limit the sound radiated from a turbulent jet to only two frequencies, it only limits the sound radiated from each eddy within the jet to two dominant frequencies. Each eddy can however have characteristic frequencies different from adjacent eddies. This two-frequency assumption for each eddy can be further supported by examining the turbulent flow structure. In the shear region of a turbulent jet, the region of maximum sound production, the eddies are stretched in the direction of the flow due to vorticity. Based on turbulence measurements, it is evident that this stretching process causes the length of the eddy in the flow

direction to be about twice its length normal to the flow. The shape of the eddy might thus be thought of as near cylindrical with its volume given by a constant times the product of its characteristic lengths. The proportionality constant must have a numerical value near one, being exactly one for a rectangle and $\pi/4$ for a cylinder. If these eddy volumes are considered to be independent sound radiators, it is likely that they will radiate predominantly at the fundamental frequencies of the volume, i.e., the two predominant frequencies are proportional to the mean eddy velocity divided by the appropriate length scales.

Using the above assumptions, Eq. (6) can be integrated over the eddy volume to yield:

$$i_t = \frac{\beta_{se} \rho^2 \omega_{se}^4 l_1 l_2 l_3}{8\pi^2 |x|^2 \rho_o a_o^5} \frac{\langle u_x^2 \rangle^2}{[(1 - M_c \cos \theta)^2 + \alpha_{se}^2 M_c^2]^{5/2}} + \frac{\beta_{sh} \rho^2 \omega_{sh}^2 l_1 l_2 l_3}{2\pi^2 |x|^2 \rho_o a_o^5} \left(\frac{\partial \langle U \rangle}{\partial r} \right)^2 \frac{\langle u_1 u_r \rangle^2 \cos^4 \theta + \langle u_r^2 \rangle^2 \sin^2 \theta \cos^2 \theta}{[(1 - M_c \cos \theta)^2 + \alpha_{sh}^2 M_c^2]^{3/2}} \quad (7)$$

where $\omega_{se} = \gamma_{se}(\langle U \rangle / l_{2,3})$ and $\omega_{sh} = \gamma_{sh}(\langle U \rangle / l_1)$. Equation (7) describes the sound intensity, spectral distribution, and directivity pattern of the sound radiated from a unit volume of turbulence in terms of self noise and shear noise components. By integrating this equation over all sound producing eddies, the total contribution to the sound reaching a point in the far field due to the self noise or shear noise can be determined independently or by integrating over slices of the jet and the sound generated as a function of location in the jet can be determined. In addition, the spectral distribution of the sound reaching a far field point can be calculated for both the self and shear noise mechanisms. The sum of these two distributions, which is the only distribution which can be measured, gives the total spectral distribution. This two-frequency method of modeling sound also allows one to predict the experimentally observed change in peak frequency as a function of angle about the jet producing the sound, i.e., low frequencies near the jet axis and higher frequencies away from the axis.

Another important aspect of this model is that it retains the physical dependence of the sound generation on the turbulence mechanism. Turbulence parameters retained in the sound model are: turbulence intensity, shear stress, length, and time scales as well as local mean density, velocity, and velocity gradients. Retention of these parameters allows one to determine effects on sound generation of initial jet turbulence levels, velocity gradients, length scales, and temperature. Because the sound has been modeled in terms of local turbulence parameters, in order to be a useful sound model, these local turbulence parameters must be predictable in terms of initial jet conditions. This brings up a very important point, i.e., are the major inaccuracies in predicting aerodynamic sound due to insufficiencies in the sound model itself or are these inaccuracies due to the use of inappropriate turbulence models? To shed some light on this question, an experiment was conducted in which detailed measurements of the appropriate turbulence parameters were measured and used to numerically integrate Eq. (7). Sound intensity and spectral distributions predicted as a result of this integration were then compared with experimental values. A discussion of this experiment and the results are presented in the following sections.

The simplest geometry which can be experimentally investigated and which will help in understanding the relationship between turbulence and sound generation is an axisymmetric free jet. In addition, the turbulent structure for this case is well known from experimental studies. Solution of Eq. (7) requires a knowledge of the following: density, mean velocity, mean velocity gradients, Reynolds stresses, length, and time scales as well as several constants. For axisymmetric jets, some information about these properties is available from the literature.

As a first approximation, the constants α_{se} and α_{sh} can be assumed equal and assigned the value 0.55 which Ribner¹⁰

found gave the best fit when compared with measurements for round jets. Assuming the sound producing eddies to be cylindrical volumes, β_{se} and β_{sh} can be set equal to $\pi/4$. The final set of constants, γ_{se} and γ_{sh} , can again as a first approximation be set equal to one another. This approximation forces the self noise to radiate at twice the frequency at which the shear noise radiates. The magnitude of γ can be approximated for an axisymmetric free jet from the time scale measurements of Chu.¹⁵ From these measurements, γ was estimated to have a magnitude of 0.3. Refinements in each of these constants could be made if additional turbulence data were available.

The least understood of the remaining flow parameters in Eq. (7) are the length scales. Since the length scales appropriate for describing the sound generation are defined in terms of integrals of the fourth-order velocity correlations they are, as yet, impossible to predict directly. Jones¹⁷ measured three of these length scales in a two-dimensional jet and showed that for this particular jet the length scales grew approximately linear with distance from the jet axis. Chu¹⁵ measured these same length scales for a circular jet. Jones compared his data with that of Chu and suggested that discrepancies between the two sets of data are due to instrumentation errors. Some instrumentation errors are indicated; however, most of the error is due to comparing length scales from jets of different geometry, size, and velocities as a function of distance from the jet exit only. Since sound is generated from history-dependent turbulent eddies, these length scales are also history dependent and thus, not comparable on a basis of distance from the jet axis alone. A more suitable correlation needs to be found. For circular jets it appears that these length scales can be written in terms of the shear layer half width (l_s). The shear layer half-width grows approximately linearly with distance downstream of a circular free jet; however, the rate of growth changes for different diameter jets. Based on very sparse data, the length scales have been related to the shear layer half width by^{15,17}

$$l_1 = 0.358l_s \quad (8a)$$

$$l_2 = l_3 = 0.179l_s \quad (8b)$$

The sound model can be further simplified for application to circular free jets, the turbulence structure being heavily studied, by assuming the correlations $\langle u_x^2 \rangle$, $\langle u_1 u_r \rangle$, and $\langle u_r^2 \rangle$ can all be modeled in terms of the single correlation $\langle u_1^2 \rangle$. This restrictive simplification need not be made; it does, however, allow all remaining variables in the model to be recovered from a one-dimensional measurement.²⁴ The error introduced by this assumption should cause the sound intensity to be slightly over predicted.

Experiment

The validity of the sound model, i.e., Eq. (7) plus the assumptions discussed above, can be demonstrated by comparing measured sound intensity, spectra, and directivity with values calculated from measured values of $\langle U \rangle$, $\partial \langle U \rangle / \partial r$, $\langle u^2 \rangle$ and l_s . A $\frac{3}{8}$ in. circular nozzle was selected for experimental study.

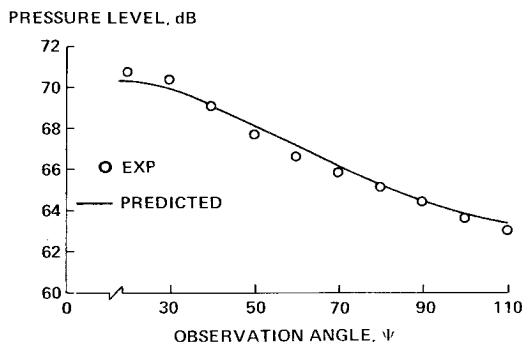


Fig. 2 Comparison of measured over-all sound pressure level and directivity with prediction made using measured turbulence data ($\frac{3}{8}$ in. diam., exit velocity 500 fps, observation distance 64.6 in.).

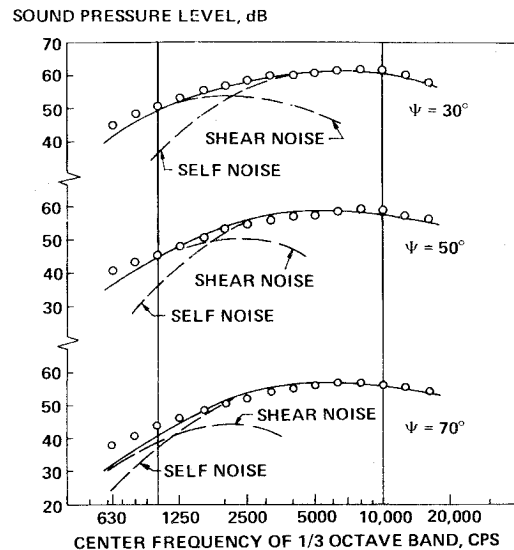


Fig. 3 Comparison of measured spectra with predictions made using measured turbulence data ($\frac{3}{8}$ in. diam., exit velocity 500 fps, observation distance 64.5 in.).

The nozzle was mounted on a three-dimensional traversing table located in one end of a $17 \times 20 \times 20$ -ft semianechoic chamber. A fixture for holding a hot-wire/film probe was attached to the base of the traversing table. Surveys of the flowfield were made by moving the nozzle relative to the fixed probe. For measurements of jet noise, a microphone boom was mounted in the ceiling and centered over the nozzle. The boom was constructed to allow the distance between the microphone and the nozzle to be varied as well as the angle between the jet centerline and the microphone. Detailed information about the facility is available.²⁴

Measurements of axial mean velocity and turbulence intensity profiles were made using a constant temperature anemometer (TSI Model 1050). Twenty-eight separate profiles were measured in the jet from the nozzle exit to twelve nozzle diameters downstream. Each profile contained an average of 20 data points.²⁴ Typical profiles are shown in Fig. 9.

Measurements of over-all sound pressure level (OASPL) were made using a condenser microphone system (B&K Model 4145-2619-2606). The sound spectra were determined at each measuring point using a $\frac{1}{3}$ -octave band analyzer (GR Model 1523-P3). These data are shown in Figs. 2 and 3.

Comparisons of Sound Predictions with Data

From the measured turbulence data, the remaining unknown flow parameters were evaluated, i.e., $\partial \langle U \rangle / \partial r$ and l_s were determined. Using these flow data in addition to the constants determined earlier, Eq. (7) was numerically evaluated. The OASPL radiated from the sound producing region of the jet is given as a function of distance and angle as

$$\text{OASPL}(R, \psi) = 2\pi a_0 \rho_0 \int_0^{z_0} \int_0^{r_0} i_1 r dr dz \quad (9)$$

Figures 2 and 3 show comparisons between measured and calculated OASPL, directivity pattern, and spectral distribution. Predictions of OASPL and directivity are seen to be in excellent agreement with the experimental data (generally less than 2% error). The frequency spectra are slightly under predicted (error generally less than 5%). Since contributions to the low frequencies come primarily from regions in the jet far downstream of the nozzle exit, the major errors in the low-frequency predictions can be attributed to integrating for only 12 diam. Inclusion of the region further downstream would have increased the low-frequency predictions while having very little effect on the OASPL predictions.

The predicted peak frequency is, also, slightly lower than

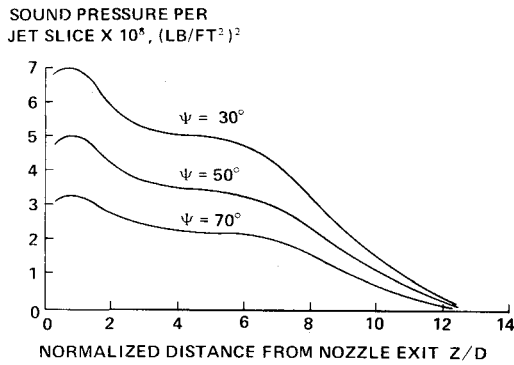


Fig. 4 Total sound radiated from successive slices of jet ($\frac{3}{8}$ in. diam., exit velocity 500 fps, observation distance 64.5 in.).

measured. Peak frequency as well as the predicted level in each $\frac{1}{3}$ -octave band are strongly dependent on the magnitude of the turbulence time and length scales. Small errors in the magnitude of these scales could also account for the inaccuracies in predicting the sound spectra.

Since the total sound radiated from the jet has been calculated by summing the sound radiated by individual eddies, the total sound reaching the observation point which originates from successive slices of the jet can be determined. The axial distribution of sound sources is shown in Fig. 4 for three separate observation angles. From this figure it can be seen that only a very small contribution to the over-all sound intensity is made by the regions of the jet beyond about 8 or 10 diam. downstream of the nozzle exit. This, however, does not imply that major contributions to the low-frequency bands cannot come from this region.

Thus, we have shown that accurate sound radiation predictions, including directivity and spectral distribution as well as the axial distribution of sound sources, can be made from measured mean and turbulence flow parameters. Next we examine the ability to model the turbulence to the required accuracy.

Turbulence Model

The turbulence model summarized below is shown to model most of the test cases used as the NASA-Langley Working Conference on Free Shear Flows,³ i.e., incompressible and compressible quiescent jets, wakes, coflowing streams of constant

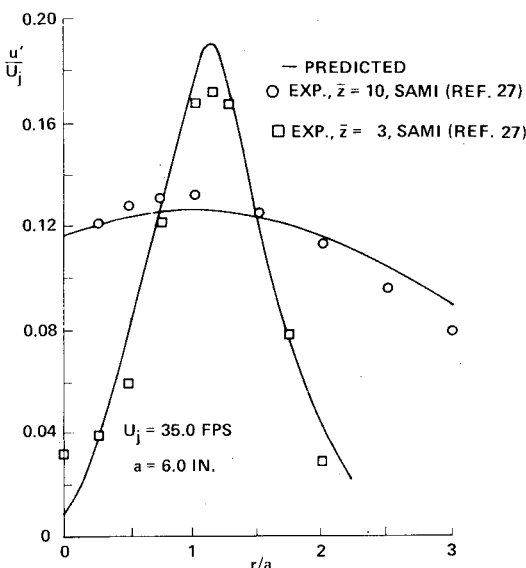


Fig. 5 Predicted and experimental axial turbulence intensity profiles at $z = 3$ and 10 for data of Sami.

density, heated jets, and coflowing streams of hydrogen mixing with air. The predictive technique used to solve the species continuity, momentum, and energy equations is a derivative of the method used by Zeiberg and Bleich,²⁵ i.e., the equations are simplified using the boundary-layer approximations, the radial velocity is eliminated using the von Mises coordinate transformation and the resulting equations are solved by employing an explicit finite difference method. An eddy viscosity approach is used, hence it is not necessary to introduce additional equations, e.g., the turbulence kinetic energy equation, and specify initial turbulence kinetic energy profiles. A unique feature of the turbulence modeling effort reported herein is the development of explicit empirical relationships for the shear correlation coefficient and turbulence intensities.

Eddy Viscosity and Turbulence Intensity Models

The eddy viscosity and axial turbulence intensity models are given below in Eqs. (10) and (11); details on how these equations were developed are reported by Zelazny²⁶

$$\epsilon_u = \frac{0.036 \int_{r_1}^2 |\rho U - \rho_e U_e| r dr}{r_u (1 + r_1/a) (1.0 + 0.6 |M_c - M_e|)} \quad (10a)$$

where

$$\frac{\epsilon}{\epsilon_u} = \frac{1.05 - 0.15\epsilon - 4.6\zeta}{1.0 + 0.05\zeta^4} \equiv G_c(\zeta) \quad \text{for } \zeta \geq 0 \quad (10b)$$

$$\frac{\epsilon}{\epsilon_u} = \frac{0.945 - 0.135\epsilon - 4.6(1 - \zeta)}{1.0 + 0.05(1 - \zeta)^7} \equiv G_c(\zeta) \quad \text{for } \zeta < 0 \quad (10c)$$

$$\zeta = (r - r_1)/(r_1 - r_1) \quad (10d)$$

and

$$\frac{u'}{U_j} = 0.49 \left[\frac{G_c \int_{r_1}^2 |\rho U - \rho_e U_e| r dr}{\rho r_u U_j^2 (1 + r_1/a) (1 + 2f) (1 + 0.6 |M_c - M_e|)} \left(\frac{\partial U}{\partial r} \right)_u \right]^{1/2} \quad (11)$$

where the time average brackets $\langle \rangle$ have been deleted with the understanding that only time averaged parameters are considered.

Equations (10) and (11) have been shown to accurately correlate data covering a wide range of flow conditions with calculations starting in the jet core. It is important to note that the expression for ϵ_u correctly reduces to the same form as Prandtl's velocity difference model as $z \rightarrow \infty$ and to Gortler's model for two-dimensional jets as $z \rightarrow 0$.

Comparisons of Turbulence Predictions with Data

Comparisons between experimental axial velocity and turbulence intensity data and their values predicted using Eqs. (10) and (11) are shown in Figs. 5 and 6. The two cases presented therein are for the data of Sami,²⁷ an incompressible quiescent jet, and Maestrello and McDaid,²⁸ a compressible quiescent jet. Comparisons for twenty-two additional cases were considered and are reported in Ref. 26. In addition, the turbulence

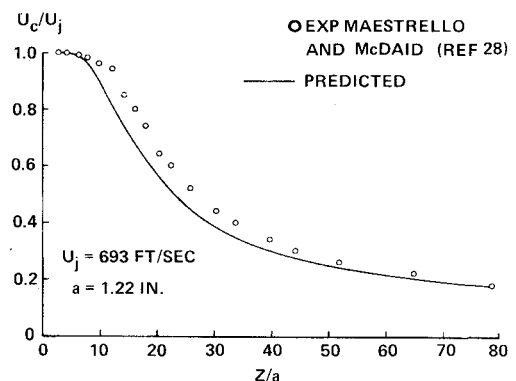


Fig. 6 Centerline velocity decay, calculations started at $z/D = 1.0$, data of Maestrello and McDaid.

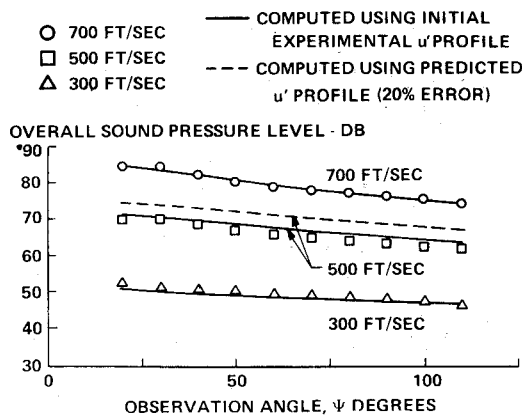


Fig. 7 Comparison between predicted and measured sound pressure level as a function of observation angle (observation distance $R = 64.5$ in.).

model was shown to accurately predict the flowfield of compressible wakes²⁹ and has been used by Holdeman³⁰ in characterizing jet engine exhaust dispersion. These results demonstrate that reasonable agreement (generally less than 20% error) of both turbulence and mean parameters can be obtained for circular and coannular jets. The significance of 20% error in turbulence intensity on predicted sound pressure levels was studied using the computationally coupled turbulence and sound models and is presented in the following section.

Turbulence and Noise Predictions

The sound and turbulence models, Eqs. (7-11) were computationally coupled in order to predict the sound spectra and pressure levels given the initial velocity profile at the jet exhaust plane. The shear layer half width, l_s , is obtained directly from the computer velocity profile and the length scales.

In previous investigations^{22,23} both the initial mean velocity and turbulence intensity profiles were required to start computations which result in the solution for the velocity and turbulence intensity throughout the entire flowfield. In most practical applications the initial turbulence intensity level is not known and is very dependent on the upstream history of the flowfield. This fact underscores a basic weakness of methods requiring initial turbulence profiles to begin flowfield predictions. To examine in detail the consequences of not having initial turbulence intensity profiles available, two sets of predictions were made for the over-all sound pressure level at various observation angles. The first set of calculations used both the initial

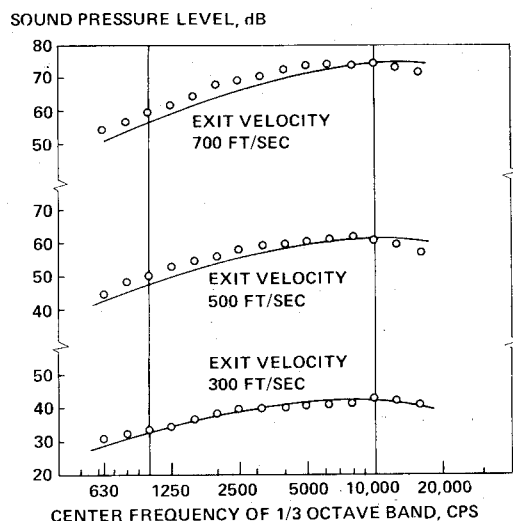


Fig. 8 Comparison between predicted and measured spectra (observation angle 30° , observation distance 64.5 in.).

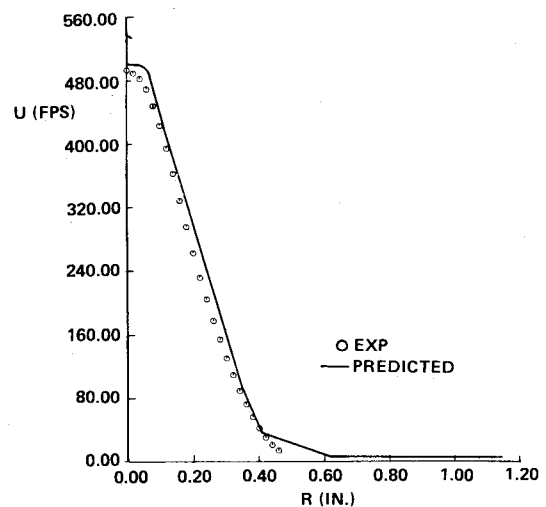


Fig. 9a Predicted and experimental axial velocity profile at $z = 2.0$ in.

experimental velocity and the turbulence intensity profiles. Results (Fig. 7) show that excellent agreement between the experimental and predicted over-all sound pressure levels were obtained for the 300, 500, and 700 fps jets. These results are comparable to results obtained using a turbulence model which requires initial turbulence intensity profiles such as a turbulence kinetic energy approach. The comparison between the predicted and experimental spectra for $\psi = 30^\circ$ and $R = 64.5$ in. is shown in Fig. 8. Note that both the shape and peak OASPL were correctly predicted although shifted toward the high frequency end of the spectra. This shift is due to the differences between the predicted and experimental length scales which are highly sensitive to small differences between the predicted and experimental mean velocity profiles.

A second set of calculations were made which represent a more realistic case where turbulence intensity levels are not available to start the calculations. Therefore, Eq. (11) was used to obtain the initial u' profile, rather than use the experimental values. As in the previous case the starting profile for mean velocity was obtained from the experimental data. Comparisons of predicted and experimental values for U and u' at $z = 2.0$ in. downstream are shown in Fig. 9a. The predicted velocity field was in excellent agreement with the experimental data; however, the length scales differed by 31% and the predicted turbulence intensity, Fig. 9b, was 20% higher than the peak experimental value and a factor of 3 lower near the centerline. The effect of the over-prediction in the peak turbulence intensity on the sound pressure level is shown in Fig. 7 as the dashed line. Note that for the 500 fps jet, the over-all sound pressure level was over the experimental value by approximately 5 db at $\psi = 90^\circ$. Similar trends were obtained for the 300 and 700 fps jets.

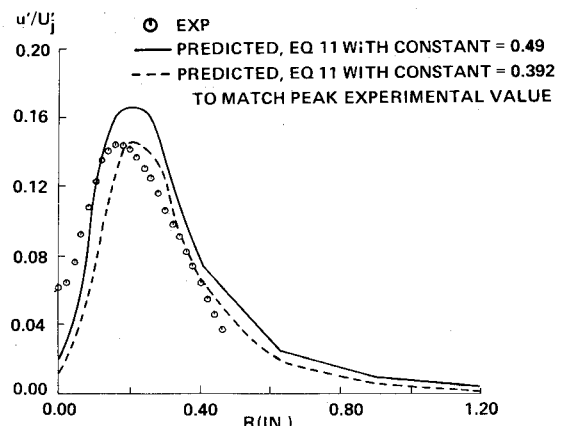


Fig. 9b Predicted and experimental axial turbulence intensity profiles at $z = 2.0$ in.

Conclusions

1) A sound model was developed, Eqs. (7) and (9), which, when given the detailed experimentally obtained flowfield, accurately predicted the sound amplitude, spectral distribution, and directivity pattern in terms of the self and shear noise components. 2) A turbulence model was developed, Eqs. (10) and (11), which accurately predicted mean velocity, shear stress, and turbulence intensity (generally less than 20% error). 3) Errors of only 20% in the predicted peak turbulence intensity level in the core region results in up to 5-db difference in the predicted over-all sound pressure level. 4) Unlike most boundary-layer type flows noise predictions are highly sensitive to inaccuracies in the starting conditions. Therefore, the key to obtaining accurate noise predictions obtained from computationally coupled turbulence and sound models is to start with accurate (at least less than 20% error) initial turbulence intensity profiles.

It is recommended that future studies of the turbulent flowfield as related to noise characterization focus on the role upstream parameters (e.g. geometry, mode of injection) have on the exit plane turbulent field.

References

- ¹ Lighthill, M. J., "On Sound Generated Aerodynamically, I," *Proceedings of the Royal Society*, Vol. A211, 1952, pp. 564-587.
- ² Lighthill, M. J., "On Sound Generated Aerodynamically, II," *Proceedings of the Royal Society*, Vol. A222, 1954, pp. 1-32.
- ³ *Proceedings of the NASA Workshop on Free Turbulent Shear Flows*, Vol. I, SP-321, July 1972, NASA.
- ⁴ Lighthill, M. J., "Sound-Generated Aerodynamically," *Proceedings of the Royal Society*, Vol. A267, pp. 147-182.
- ⁵ Csanady, G. T., "The Effect of Mean Velocity Variations on Jet Noise," *Journal of Fluid Mechanics*, Vol. 26, Sept. 1966, pp. 183-197.
- ⁶ Jones, Ian, S. F., "Aerodynamic Noise Dependent on Mean Shear," *Journal of Fluid Mechanics*, Vol. 33, July 1968, pp. 65-72.
- ⁷ Bradshaw, P. and Ferriss, D. H., "Calculation of Boundary-Layer Development Using the Turbulent Energy Equation," AERO Rept. 1217, Nov. 1966, National Physics Laboratory, England.
- ⁸ Lilley, G. M., "On the Noise From Air Jets," ARC 20, 376-N40-FM 2724, 1958, Aeronautical Research Council, London.
- ⁹ Ffowcs Williams, J. E., "The Noise from Turbulence Convected at High Speed," *Philosophical Transactions of the Royal Society (London)*, Ser. A, Vol. 255, 1963, pp. 469-503.
- ¹⁰ Ribner, H. S., "The Generation of Sound by Turbulent Jets," *Advances in Applied Mechanics*, Vol. 8, Academic Press, New York and London, 1964, pp. 103-182.
- ¹¹ Ribner, H. S., "Quadrupole Correlations Governing the Patterns of Jet Noise," *Journal of Fluid Mechanics*, Vol. 38, Aug. 1969, pp. 1-24.
- ¹² Krishnappa, G., "Estimation of the Intensity of Noise Radiated from a Subsonic Circular Jet," *Proceedings of the AFOSR (University of Toronto Institute Aerospace Sciences Symposium, Toronto, 1968)*, University of Toronto Press, Toronto, Canada, 1968.
- ¹³ Krishnappa, G., Csanady, G. T., "An Experimental Investigation of the Composition of Jet Noise," *Journal of Fluid Mechanics*, Vol. 37, June 1969, pp. 149-159.
- ¹⁴ Schubert, L. K., *Aerodynamic Noise*, University of Toronto, Institute for Aerospace Studies, Toronto, Canada, 1967, pp. 42-48.
- ¹⁵ Chu, W. T., "Turbulence Measurements Relevant to Jet Noise," Rept. 119, 1966, University of Toronto, Institute for Aerospace, Toronto, Canada.
- ¹⁶ Davies, P. O. A. L., Fisher, M. J. and Barratt, M. J., "The Characteristics of the Turbulence in the Mixing Region of a Jet," *Journal of Fluid Mechanics*, Vol. 15, March 1963, pp. 337-367.
- ¹⁷ Jones, Ian, S. F., "Fluctuating Turbulent Stresses in the Noise Producing Region of a Jet," *Journal of Fluid Mechanics*, Vol. 36, May 1969, pp. 529-543.
- ¹⁸ Bradshaw, P., "Turbulence in the Noise-Producing Region of a Circular Jet," *Journal of Fluid Mechanics*, Vol. 19, Aug. 1964, pp. 591-624.
- ¹⁹ Bradshaw, P., "The Effect of Initial Conditions on the Development of a Free Shear Layer," *Journal of Fluid Mechanics*, Vol. 26, Oct. 1966, pp. 225-236.
- ²⁰ Laurence, J. C., "Intensity, Scale, and Spectra of Turbulence in Mixing Region Free Subsonic Jet," Rept. 1292, 1956, NACA.
- ²¹ Lassiter, L. W., "Turbulence in Small Air Jets at Exit Velocities up to 705 Feet per Second," *Journal of Applied Science*, Vol. 22, Sept. 1957, pp. 349-354.
- ²² Benzakein, M. J., "A Computational Technique for Jet Aerodynamic Noise," AIAA Paper 71-583, Palo Alto, Calif. 1971.
- ²³ Knott, P. R., "Analytical and Experimental Supersonic Jet Noise Research," AIAA Paper 73-188, Washington, D.C., 1973.
- ²⁴ Moon, L. F., "Microjet Nozzle Characterization," Rept. 9500-920267, Dec. 1972, Bell Aerospace Co., Buffalo, N.Y.
- ²⁵ Zeiberg, S. L. and Bleich, G. D., "A Finite Difference Method Solution of the Laminar Hypersonic Nonequilibrium Wake," GASL-TR-338, Westbury, N.Y., Feb. 1963.
- ²⁶ Zelazny, S. W., "Modeling of Turbulent Axisymmetric Coflowing Streams and Quiescent Jets: A Review and Extension," Ph.D. dissertation, Dept. of Engineering Science, Sept. 1972, University of Buffalo, Buffalo, N.Y.
- ²⁷ Sami, S., "Velocity and Pressure Fields of a Diffusing Jet," Ph.D. dissertation, University Microfilms 67-2672, 1966, University of Iowa, Ames, Iowa, summarized in *Journal of Fluid Mechanics*, Vol. 27, 1967, pp. 231-252, and *Journal of Fluid Mechanics*, Vol. 29, July 1967, pp. 81-92.
- ²⁸ Maestrello, L. and McDaid, E., "Acoustic Characteristics of a High-Subsonic Jet," *AIAA Journal*, Vol. 9, June 1971, pp. 1058-1066.
- ²⁹ Demetriades, A., "Mean-Flow Measurements in an Axisymmetric Compressible Turbulent Wake," *AIAA Journal*, Vol. 6, March 1968, pp. 432-439.
- ³⁰ Holdeman, J. D., "Dispersioin of Turbojet Engine Exhaustion Flight," TN D-7382, Aug. 1973, NASA.